DØ Note: 3354
December 2nd, 1997

Triggers for B Physics Studies in Run II

Frédéric Stichelbaut
State University of New York at Stony Brook

Andrzej Zieminski
Indiana University, Bloomington

Meenakshi Narain
Fermi National Accelerator Laboratory

Abstract

The upgrade of the DØ detector foreseen for Run II will enhance the capabilities to study the B sector, allowing searches for CP violation and B_s mixing. A crucial issue in these studies is the possibility to trigger on the interesting events. We investigate the trigger efficiency that could be obtained for various channels with the current configuration of the trigger system for Run II. We then evaluate the benefits for B physics that could result from the implementation of a Silicon Track Trigger preprocessor at level two. The B_s mixing and CP violation studies are reexamined taking into account the expected trigger efficiencies.

1 Introduction

The increase of the Tevatron luminosity to 2×10^{32} cm^{-2}s^{-1} for Run II will lead to a huge $b\bar{b}$ production rate of 10 KHz. This high statistics B sample is expected to enable the study of low branching ratio B decays, the search for CP violation in the B sector or the observation of B_s mixing.

The most promising way to determine the angle β of the unitarity triangle is to measure the CP asymmetry of the decay mode $B_d^\circ \to K_s + J/\psi$ [1]. A recent study of this channel [2] concluded that the parameter $\sin 2\beta$ could be measured in DØ with an accuracy of $0.12/\sqrt{\epsilon}$ for an integrated luminosity of 2 fb^{-1}, where ϵ represents the trigger and reconstruction efficiency for events within the geometrical and kinematical acceptance.

The B_s mixing can be studied in Run II by looking for decay modes like $B_s^\circ \to D_s^- + \ell^+ + X$ or $B_s^\circ \to D_s^- + n\pi^\pm$, where $D_s^- \to K^+K^-\pi^-$. A simulation of the DØ upgrade detector shows that a sensitivity for x_s up to 20 could be reached [3].

With its extended muon coverage and excellent muon identification, DØ can easily trigger on the semileptonic decay of B mesons into muons. Thanks to the installation of the central and forward preshowers in Run II, DØ should also be able to trigger on electrons. But, because of the limited bandwith available at the level one (10 kHz) and level two (1 kHz) of the current trigger system, and the huge amount of low energy leptons expected in Run II, the rate of low threshold lepton triggers could rapidly become unacceptable. Solving this problem by prescaling these triggers or rising their p_T threshold could result in a dramatic reduction of the B sample statistics and forbid some crucial measurements. Another solution could be a level 2 trigger preprocessor using the data of the Silicon Vertex Detector (SVX) that would allow to trigger on events containing tracks with large impact parameters in the transversal plane, coming from the decay of B/D mesons. This device would allow to enrich the collected raw data set with events containing b quarks while keeping the background trigger rate at an acceptable level. The physics motivations for this Silicon Track Trigger (STT) were presented in [4].

In this note, we present the background rates and the trigger efficiencies expected for various $b\bar{b}$ samples in the framework of the present Run II trigger scheme. We then investigate the benefits that could be obtained from a STT preprocessor.

The Monte-Carlo samples used in this analysis are described in section 2. Some properties of the $b\bar{b}$ events are presented in section 3. The $b\bar{b}$ trigger efficiencies obtained with the current trigger design are discussed in section 4. The use of the STT for B physics is presented in section 5. Finally, the feasibility of some B physics studies is reviewed in section 6 in view of the expected trigger efficiencies.

2 Monte-Carlo Samples

This study is based on various samples of $b\bar{b}$ Monte-Carlo events generated with ISAJET at $\sqrt{s} = 2$ TeV and giving muons or electrons in the final state. The detector response was simulated with the FEB97 version of UPG_GEANT, corresponding to the current baseline of the silicon vertex detector geometry with six 4-layer barrels. Ntuples were produced with the September 4th, 1997 version of the UPG_TRG ntuples maker. The samples with muons in the final state are the following:

- $Q\bar{Q} \to \mu\mu X$. The events were generated with NLO in 3 bins of p_T^b: 2–3, 3–5 and 5–80. Only events with 2 muons satisfying the acceptance cuts $p_T^\mu > 1.5$ GeV/c and $\mid \eta^\mu \mid < 2$ were kept for Geanting. These 3 bins correspond to a total of 45K events, 5.2 K belonging to the first two bins. To check the p_T^b spectrum of these events, we compared their differential cross section $d\sigma^b/dp_T^b$ to the MNR [5] prediction at $\sqrt{s} = 2$ TeV. To obtain a good agreement, we were forced to remove the last p_T^b bin from our sample because it gives a much too hard spectrum compared to MNR. Using only the first two p_T^b bins, the ISAJET and MNR p_T^b spectra are shown in Fig. 1, both spectra being normalized to the MNR total cross section for $p_T^b \geq 6$ GeV/c and $\mid y^b \mid \leq 1$. These two spectra are in good agreement. The absolute normalization of this sample was obtained by using the DØ measurements of the inclusive b-quark cross section at 1.8 TeV (see section 5.1). We verified that, including the last p_T^b bin to our sample, our results are changed by 20%.

- $b \to J/\psi + X$ with $J/\psi \to \mu^+\mu^-$. These events were generated with ISAJET, using the leading order only and a single p_T^b bin between 4 and 80 GeV/c. The events are accepted for Geanting if both muons had $p_T > 1.5$ GeV/c and $\mid \eta \mid < 2$. The normalization of this sample was done using the CDF measurement of J/ψ production cross section at 1.8 TeV.
- Direct J/ψ events generated with ISAJET LO, with $p_T(J/\psi)$ between 3 and 80 GeV/c. The same muon cuts as for the previous sample were applied and the CDF measurement of prompt J/ψ production at 1.8 TeV was used for normalization.
- $B_d^\circ \to K_s + J/\psi$ with $J/\psi \to \mu^+\mu^-$. The $b/\bar{b}$ jets were required to have a transverse momentum ranging from 4 to 80 GeV. Events where a B° meson was produced from the $\bar{b}$ fragmentation were kept. This meson was forced to decay into $K_s\, J/\psi$, the J/ψ decaying itself into a muon pair. A total sample of 9760 events was generated, each event corresponding to a weight of 1 pb $\times \frac{Br(b \to J/\psi + K_s)}{Br(b \to J/\psi + X)}$.
- $B_s^\circ \to D_s^- + \mu^+ + \nu_\mu$. The $b/\bar{b}$ jets were required to have a transverse momentum ranging from 2 to 100 GeV. Events where one of the b's hadronizes into B_s are kept. The other b must have a semileptonic decay into a muon. The B_s meson is forced to decay into $D_s^-\, \mu^+\, \nu_\mu$, followed by $D_s^- \to \phi^\circ + \pi^-$ and $\phi^\circ \to K^+K^-$. This sample contains 2275 events and corresponds to an integrated luminosity of 20 pb^{-1}.
- $B_s^\circ \to D_s^- + 3\pi^\pm$. The $b/\bar{b}$ jets were required to have a transverse momentum ranging from 2 to 100 GeV. Events where one of the b's hadronizes into B_s are kept. The other b must have a semileptonic decay into a muon. The B_s meson is forced to decay into $D_s^- + 3\pi^\pm$, followed by the same D_s decay mode as above. This sample contains 2323 events, corresponding to an integrated luminosity of 20 pb^{-1}.

For b quarks giving electrons, we used the following samples:

- $Q\bar{Q} \to eeX$. The events were generated with NLO in one bin of p_T^b between 5 and 80 GeV/c. Only events with 2 electrons satisfying the acceptance cuts $p_T > 1.5$ GeV/c and $\mid \eta^\mu \mid < 2$ were kept for Geanting.
- $b \to J/\psi + X$ with $J/\psi \to e^+e^-$. These events were generated with ISAJET, using the leading order only and a single p_T^b bin between 4 and 80 GeV/c. Both electrons had to satisfy $p_T > 1.5$ GeV/c and $\mid \eta \mid < 2$.

To estimate the QCD background trigger rates, we used the official dijet events produced by the upgrade trigger group. They correspond to TWOJET ISAJET events generated in 6 p_T intervals (2–5, 5–10, 10–20, 40–80 and 80–500) with 1, 3, 5 or 7 additional minimum bias interactions (p_T between 1 and 100 GeV/c) per event. They were simulated with the AUG96 version of UPG_GEANT (7 barrels) and ntuples were produced with the latest version of UPG_TRG. The background trigger rates were computed with the assumptions of an instantaneous luminosity of 2×10^{32} cm^{-2}s^{-1}, a beam crossing time interval of 132 ns and a dijet total cross section of 57 mb. Each sample contained about 1000 events, some rate calculation could suffer from large fluctuation due to the small number of selected events. It is also accepted that the absolute rates obtained from these samples could be underestimated by a factor up to 2.

3 Some Properties of the $b\bar{b}$ Samples

Some properties of the $B_d^\circ \rightarrow K_s + J/\psi$ events are illustrated in Fig. 2. The average number of charged particles produced with $p_T \geq 0.5$ GeV/c and $\mid \eta \mid \leq 2.2$ is about 16, 25% of them coming from the decay of B mesons. The primary vertex (PV) position is (0.,0.,z_0), with z_0 generated following a Gaussian distribution with a width of 25 cm. The charged particle multiplicity is greatly reduced when kinematical cuts are applied to take into account the acceptance of the CFT. Requiring $p_T > 1.5$ GeV/c, $\mid \eta \mid \leq 1.6$ and $\mid z_0 \mid \leq 30$ cm, the average charged multiplicity drops to 2.6 in case of the $B_d^\circ \rightarrow K_s + J/\psi$ events, as shown in Fig. 3. This average multiplicity is further reduced to 2.4 and 2.1 for the $B_s^\circ \rightarrow D_s^- + \mu^+ + \nu_\mu$ and $B_s^\circ \rightarrow D_s^- + 3\pi^\pm$ events, respectively. Most of the particles surviving after the cuts come from the B mesons decay: 84.2% in case of the $K_s + J/\psi$ sample and 82.8% for the $B_s \rightarrow D_s$ events. These properties are similar for the inclusive $Q\bar{Q}$ events, with an average charged multiplicity of 2.6 after acceptance cuts, 80.9% of the charged particles being produced in the decay of the B mesons.

In summary, the $b\bar{b}$ events are characterized by a very low multiplicity of charged particles within the acceptance of the CFT but, as most of these particles come from B mesons decay, they should possess large impact parameters. A STT should thus be quite efficient to select these events.

4 Efficiency and Rate of Standard Triggers

The first triggers considered in this study are based on the CFT, calorimeter and muon chambers information. They correspond to the standard muon triggers defined in the analysis code provided by the upgrade trigger group and are listed in appendix A. Their background rate is shown at level one (L1) and level two (L2) in Table 1, together with the number of triggered events for some of the $b\bar{b}$ samples giving muons.

One can observe that the muon triggers based on XL muons (MUMAX1 and DIMU1) give a rather large L2 trigger rate, representing 10 to 30% of the available bandwith. These rates are reduced by a factor 20 to 50 when XT muons are used instead of XL. One also notice that the jets+muons triggers give a very poor efficiency which is below 1% for the three $b\bar{b}$ samples studied. As these triggers already represent a non-negligeable fraction of the L2 bandwith, their rate would rapidly become unacceptable if the jet E_T or muon p_T threshold was reduced.

For the $b\bar{b}$ events decaying to electrons, we obtain the background rate and the signal efficiency shown in Table 2 using the dielectron trigger DIELEC described in

Table 1: Background rate and number of triggered events for various standard muon triggers.

	Bgd. (Hz)		$D_s^- + \mu^+$		$D_s^- + 3\pi^\pm$		$K_s + J/\psi$		$Q\bar{Q} \to \mu\mu$	
N$_{generated}$			2275		2323		9760		5183	
Trigger	L1	L2	L1	L2	L1	L2	L1	L2	L1	L2
1–MUMAX1	714	339	117	16	41	5	1211	228	548	151
2–MUMAX2	13.0	6.5	90	13	31	4	911	171	375	103
3–DIMU1	147	146	191	95	2	1	1904	1089	567	341
4–DIMU2	6.2	6.2	97	47	0	0	1178	718	353	221
5–MUJET	75	47	7	3	4	1	35	12	100	76
6–DIMUJ	102	102	14	11	5	3	148	90	234	215

appendix A. The large background rate subsisting at L2 can be reduced by requiring a match between a CFT track and an electromagnetic cluster, asking for an absolute difference in azimuthal angle less than 0.15 radians. This matching requirement reduces the background rate by a factor 2.4 and has an efficiency of 66% for the J/ψ events.

Table 2: Background rate and number of triggered events for the dielectron triggers.

Trigger	Bgd. (Hz)	$b \to J/\psi$	$Q\bar{Q} \to ee$
$N_{generated}$		11496	3253
DIELEC–L1	3526	850	223
DIELEC–L2	275	309	72
DIELEC+CFT match	117	205	

Combining triggers 1, 3, 5 and 6 in Table 1, one obtains a total trigger efficiency of 4.9%, 0.4% and 12.2% for the $D_s^- + \mu^+$, $D_s^- + 3\pi^\pm$ and $K_s + J/\psi$ events, respectively. In view of these rather low trigger efficiencies, we tried to find better single muon and dimuon triggers by varying the trigger definition.

4.1 Single Muon Triggers

In Table 3, we present the trigger rates and efficiencies obtained for various definitions of the single muon trigger. Each trigger is labelled by two letters and one number:

- The first letter refers to the covered region:
  - C = Central, with $|\eta| \leq 1$;
  - A = All, with $|\eta| \leq 1.5$;
  - X = eXtended, with $|\eta| \leq 2$.
- The second letter describes the tag criterium:
  - L stands for Loose tag;
  - M stands for Medium tag;
  - T stands for Tight tag.
- Finally, the number is used to define the muon p_T threshold:

- 1 corresponds to an approximative threshold of 2 GeV/c;
- 2 corresponds to an approximative threshold of 4 GeV/c;
- 3 corresponds to an approximative threshold of 7 GeV/c.

For the L1 trigger, we simply require at least one muon satisfying our conditions. For L2, we demand a confirmation in the CFT, asking for **at least two** CFT tracks with the same p_T threshold than L1. In the last 2 columns, we give the efficiency for $Q\bar{Q}$ events with a single muon ($p_T \geq 1.5$ GeV/c and $\mid \eta \mid \leq 2$) obtained by dividing the number of selected $Q\bar{Q} \to \mu\mu$ events by 2.

Table 3: Background rates and signal efficiencies for single muon triggers.

Trigger	Bgd. (Hz)		$D_s^- + \mu^+$ (%)		$D_s^- + 3\pi^{\pm}$ (%)		$K_s + J/\psi$ (%)		$Q\bar{Q} \to \mu$ (%)	
	L1	L2	L1	L2	L1	L2	L1	L2	L1	L2
XL3	714	339	5.1	0.7	1.8	0.2	12.4	2.3	10.6	2.9
XM3	13.5	6.9	4.4	0.8	1.4	0.2	10.8	2.0	8.4	2.4
XT3	13.0	6.5	4.0	0.6	1.3	0.2	9.3	1.8	7.2	1.9
XL2	2856	2066	17.7	8.4	7.0	3.0	31.7	16.8	22.2	13.0
XM2	38.6	21.0	11.8	5.7	4.6	2.0	23.9	13.5	16.1	9.7
XT2	36.3	20.3	10.6	5.1	4.1	1.9	20.1	11.4	13.4	8.0
CL3	705	334	4.4	0.7	1.5	0.2	11.1	2.3	9.6	2.8
CM3	4.5	2.3	3.7	0.8	1.2	0.2	9.6	1.9	7.6	2.3
CT3	4.2	2.05	3.2	0.6	1.1	0.2	8.0	1.7	6.4	1.9
CL2	2803	2028	17.0	8.3	6.7	3.0	30.3	16.6	21.1	12.6
CM2	26.3	10.7	11.3	5.6	4.3	2.0	22.7	13.4	15.2	9.5
CT2	24.1	10.2	9.9	5.0	3.8	1.9	18.8	11.2	12.3	7.9

On base of these results, several observations can be made:

- The GEANT version we used does not contain a complete description of the muon detector foreseen for Run II [6]. That explains the weak improvement in the signal efficiency obtained by going from the central to the extended region. The muon trigger efficiency is limited to 60% for $1.5 <\mid \eta \mid< 2$ with this version and is expected to increase up to 85% in the final version.
- The use of the CFT trigger at L2 implies a significant reduction of the signal efficiency, which is not compensated by a similar reduction of the background rate. For example, the efficiency obtained for the $D_s^- + \mu^+$ events with the XL3 trigger is reduced by a factor 7 between L1 and L2, while the background trigger rate is only divided by 2. For the XL2 trigger, the signal efficiency is reduced by a factor 2 while the background rate is lowered by 30%. We conclude that the CFT confirmation added to the single muon trigger at L2 significantly affects the trigger efficiency of the low multiplicity $b\bar{b}$ events and is not very useful.
- The triggers based on the loose tag give very large background rates. Even with the 7 GeV/c threshold, these rates would be unacceptable at L2 .
- The background rate reduction obtained by replacing the medium tag by the tight tag is almost marginal. Both the trigger rate and the signal efficiency are reduced by a similar amount.

- The signal efficiencies obtained with the 7 GeV/c threshold are low, whatever type of coverage or tag is considered.
- We have not included in Table 3 the results obtained for the lowest p_T threshold (2 GeV/c) because the background rates are much too large.

These considerations lead us to the conclusion that the most interesting single muon trigger is probably XM2 without CFT confirmation. It gives a reasonable background trigger rate of 38.6 Hz and efficiencies ranging between 4.6% ($D_s^- + 3\pi^\pm$) and 23.9% ($K_s + J/\psi$) for the $b\bar{b}$ events.

4.2 Dimuon Triggers

In Table 4, we present the background rates and efficiencies obtained for various configurations of the dimuon trigger. Following the observations made with the single muon triggers, we do not use any CFT trigger information at L2 so that L1 and L2 are strictly the same.

Table 4: Background rates and signal efficiencies for dimuon triggers.

Trigger	Bgd. (Hz)	$D_s^- + \mu^+$ (%)	$K_s + J/\psi$ (%)	$Q\bar{Q} \to \mu\mu$ (%)
(CL1,CL1)	341	10.3	23.4	14.5
(CL1,CL2)	107	5.2	14.6	8.4
(CM1,CM1)	341	10.3	23.4	14.5
(CM1,CM2)	1.3	3.3	10.2	5.8
(CT1,CT1)	272	8.2	20.1	12.7
(CT1,CT2)	1.1	2.5	8.8	5.3
(AL1,AL1)	2098	13.7	28.9	19.9
(AL1,AL2)	116	6.2	16.6	9.6
(AM1,AM1)	2098	13.7	28.9	19.9
(AM1,AM2)	3.1	3.7	11.6	6.5
(AT1,AT1)	2021	11.1	25.1	18.2
(AT1,AT2)	2.9	2.9	10.0	5.9
(XL1,XL1)	16860	25.4	41.9	33.1
(XL1,XL2)	147	8.4	19.5	10.9
(XM1,XM1)	16860	25.4	41.9	33.1
(XM1,XM2)	6.4	5.1	13.9	
(XT1,XT1)	16780	22.1	38.1	30.7
(XT1,XT2)	6.2	4.3	12.1	6.8

The dimuon triggers limited to the central region give acceptable rates at L1. The triggers with the same threshold on both muons give a large trigger rate compared to the L2 limit (1 kHz) and additional rejection would be needed at L2. When one of the muons is requested to have a p_T greater than 4 GeV/c, the trigger rates are then a few Hz for the medium and tight tags but the J/ψ efficiency is limited to 14%. Therefore, the trigger (XM1,XM2) would be the most adequate, with a background rate limited to 6.4 Hz, and efficiencies of 5.1% and 13.9% for $D_s^- + \mu^+$ and $K_s + J/\psi$

events, respectively. Depending upon the bandwith allocated to B-Physics at L1, the (CM1,CM1) trigger, or even (AM1,AM1), could be an interesting option, provided that some background rate reduction is obtained at L2 by additional means.

4.3 Estimation of Absolute Signal Rates

To determine the $Q\bar{Q}$ contribution to the single muon and dimuon trigger rates, we need to know the weights corresponding to a single muon or dimuon event. To obtain this normalisation, we start from the inclusive $b\bar{b}$ cross section measured by DØ at 1.8 TeV, i.e. $\sigma^b = 7.2$ μb for $p_T^b > 6$ GeV/c and $\mid \eta^b \mid < 1$ [8]. This cross section is exactly a factor 2 larger than the MNR prediction at $\sqrt{s} = 1.8$ TeV for the same acceptance cuts. As the MNR prediction at $\sqrt{s} = 2$ TeV is 4.0 μb, the measured cross section needs to be multiplied by 1.11 to take into account the increase in energy foreseen for Run II. The branching ratio for $b\bar{b} \to \mu\mu$ being 6% and the number of b quarks generated with $p_T^b > 6$ GeV/c and $\mid y^b \mid < 1$ being equal to 11160 before muon acceptance cuts, the weight for a dimuon event is equal to 43 pb. To obtain the single muon event weight, the dimuon branching ratio needs to be replaced by the single muon branching ratio (20%), and a correction factor must be introduced to take into account the fact that the acceptance cuts were applied on both muons. This weight is then equal to 375 pb. Given the number of events selected with the XM2 trigger, we find that the rate of single muon events coming from $Q\bar{Q}$ would be 31 Hz. This irreducible single muon trigger rate must be compared to the 38.6 Hz rate found for the dijet events, suggesting that this background rate is perhaps underestimated by a significant factor.

To estimate the contribution from J/ψ production to the single muon trigger rate, we normalized the relevant Monte Carlo samples ($b \to J/\psi + X$ and prompt J/ψ's) to the CDF measurement of the J/ψ cross sections in the kinematic range $p_T(J/\psi) > 5$ GeV/c and $\mid \eta(J/\psi) \mid < 0.6$ [9]. With this normalization we find that the irreducible L1 trigger rate (XM2) for signal events is 2.0 Hz for prompt J/ψ's and 0.5 Hz for J/ψ's from b-quark decays (J/ψ with $p_T(J/\psi) > 3$ GeV/c and $\mid \eta(J/\psi) \mid < 1.5$).

5 Impact of a Silicon Track Trigger

In the previous section, we have investigated the background rates and signal efficiencies obtained from standard triggers based on the current design of the trigger system. In this section, we want to determine the benefits that could result from the use of a silicon track trigger.

We use the methods previously developped to study $t\bar{t}$ events and described in [7]:

- The STT tracks with a reduced $\chi^2 > 4$ are refit after dropping the hit with the largest contribution to the χ^2;
- The tracks must satisfy some quality cuts: hits in at least 3 layers of the silicon vertex detector and track fit $\chi^2 \leq 4$;
- The error on the track impact parameter B is determined from the relation:

$$\sigma_B^2 = \sigma_0^2 + (\frac{\alpha_{MS}}{p_T})^2 \qquad (1)$$

with $\sigma_0 = 12.6\ \mu$m and $\alpha_{MS} = 49.7$ (GeV/c).μm;

- The impact parameter significance, S_B, is defined as:

$$S_B = \frac{B}{\sigma_B}. \tag{2}$$

The S_B distribution obtained for STT tracks coming from the primary vertex in $B_d^\circ \to K_s + J/\psi$ events is shown in Fig. 4. A Gaussian fit gives a width close to 1, demonstrating that the impact parameter errors are correctly estimated. The difference between the S_B distributions obtained from primary tracks and tracks coming from a B or D meson decay is striking, as shown in Fig. 5. This clearly demonstrates that large S_B values are associated to tracks coming from secondary vertices.

In Fig. 6 is shown the multiplicity of STT tracks obtained after the quality cuts only and when a significance greater than 2 is required. Despite the low multiplicity of charged particles in these $b\bar{b}$ events, a large fraction of them contains at least one track with a significance greater than 2. Fig. 7 illustrates the efficiency obtained by requiring the presence of a minimum number of tracks with absolute significance above a given threshold S_{min}. Requiring at least one track with $\mid S_B \mid \geq 2$ gives an efficiency of 71% for the $B_d^\circ \to K_s + J/\psi$ events but only 46.2% for the $B_s^\circ \to D_s^- + 3\pi^\pm$ events. This efficiency difference increases with S_{min}. One should notice that about 15% of the $K_s + J/\psi$ events are rejected when requiring at least one track in the STT even in the absence of cuts on S_B. They mainly correspond to events produced outside the acceptance of the SVX due to a large value of the z position of the PV. Even if these events are selected by a muon trigger, they will probably be rejected either at L3 or by the offline analysis because of the absence of tracks in the SVX.

In definition (2) of the impact parameter significance, we have only considered the contribution of the SVX resolution and the multiple scattering to the impact parameter resolution. Another important contribution is the uncertainty affecting the position of the primary vertex in the transversal plane. To simulate this effect, we can replace this definition of S_B by:

$$\tilde{S}_B = \frac{B + B_{PV}}{\sqrt{\sigma_B^2 + \sigma_{PV}^2}} \tag{3}$$

where σ_{PV} is the uncertainty on the PV position and B_{PV} is a correction to the impact parameters valid for all the tracks belonging to the same event, generated along a Gaussian distribution of width σ_{PV}.

We have considered 4 cases where the STT could bring some improvement to the present trigger scheme:

1. Single muon trigger + STT;
2. Dimuon trigger + STT;
3. Dielectron trigger + STT;
4. Dielectron trigger + E_T/p_T matching using the p_T resulting from the STT track fit.

5.1 Single Muon Triggers + STT

We show in Fig. 8 the trigger efficiency obtained for $K_s + J/\psi$ events versus the background rate for various single muon triggers defined in the previous section (see Table 3). The circles correspond to a trigger obtained by combining XL2 at L1 with the STT at L2, each point corresponding to a different cut on S_{min}. This combination does not allow to obtain any improvement with respect to the XM2 trigger.

In case the background rate obtained with the XM2 trigger would be underestimated by a factor 2 or more, this trigger would need to be prescaled to maintain an acceptable rate. We demonstrate in Fig. 9 that the STT would then represent a much better alternative. This figure shows the background rate and the $Q\bar{Q} \to \mu\mu$ trigger efficiency for the XM2+STT trigger. The background rate and the efficiency are computed relative to the XM2 term. Requiring at least 1 track with an absolute impact parameter significance greater than 5 permits the reduction of the background rate by a factor 10 while keeping 60% of the signal. As pointed out previously, 15% of the $Q\bar{Q} \to \mu\mu$ events are rejected when one STT track is requested. Removing these useless events from the XM2 sample, the relative efficiency of the STT trigger becomes 70% instead of 60%.

Using the procedure described in section 4.3 to compute the signal rates, we find a rate of 18.3 Hz for the $Q\bar{Q}$ events when asking for at least one STT track with $\mid S_B \mid \geq 5$. This number is inconsistent with the background rate of 3.6 Hz obtained with the same criterium, the background events being supposed to contain the $Q\bar{Q}$ events. This discrepancy should lead us to consider with precaution the background rates obtained with the standard trigger ntuples.

In Fig. 10 we show how a primary vertex smearing of 30 μm introduced in relation (3) would affect the background rate and the $K_s + J/\psi$ efficiency for the XM2+STT trigger. Although the signal efficiency is reduced compared to the ideal case for the same S_{min} cut, this reduction is compensated by a strong background rate reduction. For a background rate reduction factor of 10, the relative signal efficiency remains above 50%, compared to 60% with no PV smearing.

Finally, we have studied the effect of the STT trigger on the separation of the J/ψ signal due to b-quark decays from the prompt J/ψ production. In case we need to suppress the prompt J/ψ signal, requiring at least one track with $\mid S_B \mid > 2.5$ provides a factor 7 reduction at the 30% cost to the no-prompt J/ψ signal.

5.2 Dimuon Triggers + STT

In Fig. 11, we plot the trigger efficiency obtained for $K_s + J/\psi$ events versus the background rate for various dimuon triggers in the central region (see Table 4). The circles correspond to a trigger obtained by combining (CT1,CT1) at L1 and the STT at L2, each point corresponding to a different cut on S_{min}. Requiring at least one track with $\mid S_B \mid > 2.5$ allows to reach a background rate below 10 Hz with a signal efficiency of 15%. For the same efficiency, this is a factor 14 reduction of the trigger rate with respect to the (CL1,CL2) trigger. Compared to the (CM1,CM2) trigger, the use of the STT allows to increase the efficiency by 50% while keeping a low background rate. Using the same argument as before about reconstructable events, the gain in efficiency would be as large as 75%.

In Fig. 12, we plot the trigger efficiency obtained for $B_s^\circ \to D_s^- + \mu^+ + \nu_\mu$ events versus the background rate for the same dimuon triggers than in Fig. 11. As in the previous case, the addition of the STT to the (CT1,CT1) dimuon trigger allows to increase the trigger efficiency by more than 50% ($\sim$ 95% for reconstructable events) and to keep the trigger rate below 10 Hz.

5.3 Summary of Triggering Scheme for Muons

We have summarized in Table 5 the background rate and signal efficiency obtained for various muon trigger configurations giving acceptable L2 trigger rates.

Table 5: Background rate and signal efficiency for various muon triggers.

Trigger	Bgd. (Hz)	$K_s + J/\psi$ (%)	$D_s^- + \mu^+$ (%)	$D_s^- + 3\pi^\pm$ (%)
DIMU2	6.2	7.4	2.1	0.0
(XM1,XM2)	6.4	13.9	5.1	0.0
(CM1,CM2)	1.3	10.2	3.3	0.0
(CT1,CT1) +STT($\mid S_B \mid \geq 2.5$)	7.6	14.9	5.5	0.3
XM2	38.6	23.9	11.8	4.6
XM2+CFT	21.0	13.5	5.7	2.0
XM2+STT($\mid S_B \mid \geq 2.5$)	13.2	17.3	7.3	2.5
XM2+STT($\mid S_B \mid \geq 3.5$)	5.6	16.0	6.2	2.0
XM2.OR. (CT1,CT1)+STT($\mid S_B \mid \geq 2.5$)	45.0	31.9	15.6	4.9
(XM2.OR.(CT1,CT1)) +STT($\mid S_B \mid \geq 2.5$)	19.6	25.2	11.0	2.7
(XM2.OR.(CT1,CT1)) +STT($\mid S_B \mid \geq 3.5$)	11.5	23.2	9.2	2.2

For the dimuon triggers, the best signal efficiency is obtained with the (CT1,CT1)+STT combination. However, the efficiency gain is small when compared to the (XM1,XM2) trigger efficiency.

For the single muon triggers, the STT provides a better rejection of the background than the CFT while preserving a better signal efficiency.

Finally, one should notice that the (XM1,XM2) or (CM1,CM2) triggers select events already contained in the XM2 sample. On the contrary, the (CT1,CT1)+STT combination allows to increase the selected event sample with respect to XM2. This is demonstrated in the bottom part of Table 5 with the trigger combination XM2.OR.[(CT1,CT1)+STT]. For a moderate increase of the background rate (16%), the $B_d^\circ \to K_s + J/\psi$ and $B_s^\circ \to D_s^- + \mu^+ + \nu_\mu$ trigger efficiencies both increase by about 33% with respect to XM2 efficiencies. The combination [XM2.OR.(CT1,CT1)] +STT(2.5) reduces the background rate to 19.6 Hz and provides a 25.2% efficiency for $K_s + J/\psi$ events.

5.4 Dielectron Trigger + STT

The STT could be used to reduce the background rate of the DIELEC trigger presented in section 3 (see Table 2). We start from the DIELEC trigger as defined in appendix A and, instead of imposing a CFT match, we add the STT at L2. The signal efficiency and background rejection factor for this trigger combination are shown in Fig. 13. Requiring at least 1 track with $\mid S_B \mid \geq 2.5$, we obtain a reduction factor of 2.7 for the background rate and an efficiency of 65% for the J/ψ events relative to the DIELEC trigger. These results are similar to the ones obtained with the CFT matching requirement. However, the rate would still be of the order of 100 Hz and some prescaling could be needed. The STT would then offer an elegant alternative to this prescaling: requiring at least two tracks with $\mid S_B \mid \geq 2$, the background rate could be reduced by a factor 10 while the $J/\psi \rightarrow ee$ sample would only be reduced by a factor 2.5. The STT trigger is probably the only way to obtain such large background reduction factors while keeping the signal unprescaled.

5.5 Dielectron Trigger + E_T/p_T Matching

We have investigated the possibility of using some E_T/p_T measurement at L2. This study used single electron events in addition to the $J/\psi \rightarrow ee$ events previously described to determine the efficiency of the E_T/p_T matching at L2.

As the precise information on the p_T of the track provided by the CFT at L2 is still under discussion, we carry out this analysis with two different definitions of the CFT-p_T for the track. The two ways of computing the CFT momentum are:

(a) Use fibers in inner and outer layer only (available at L2);

(b) Use p_t^{min} & p_t^{max} the momentum limits from the CFT track equation at L1
$$\Rightarrow \frac{1}{p_t} = \frac{1}{2}\left(\frac{1}{p_t^{min}} + \frac{1}{p_t^{max}}\right)$$

In Fig. 14 we compare the E_T/p_T distributions obtained from 5 GeV single electrons for tracks with SVX information and without SVX information using both CFT-p_T definitions. The same distributions for 20 GeV single electrons are shown in Fig. 15. Given the fact that it is currently not possible to compute CFT-p_T with definition (b), the SVX information gives a factor 2 improvement on the E_T/p_T resolution for high p_T electrons.

In Table 6, we show the rejection and efficiency obtained for two types of p_T definition relative to the standard 'isolated electron' definition [1]. The addition of the SVX information to the electron p_T determination allows to increase the background rejection factor while leaving the efficiency almost unaffected.

This E_T/p_T matching requirement could be used to reduce the background rate for the DIELEC trigger described in section 3 (see Table 2). In addition to the CFT track match introduced at L2, we also require that the quantity E_T/p_T falls between 0.5 and 1.3. To apply this criterium, we use the p_T obtained by the STT track fit. If this track fit fails, we use the p_T corresponding to the CFT track matched to the electromagnetic cluster, using definition (a). With this additional criterium, the background trigger

[1] An isolated electron is defined by an electromagnetic fraction greater than 95% and an isolation fraction greater than 80%

Table 6: Background rejection and efficiency of E_T/p_T matching relative to the standard isolated electron definition.

	$p_T(ele) = 20$ GeV		$p_T(ele) = 5$ GeV	
p_T type	Eff. (%)	Bkg Rej.	Eff. (%)	Bkg Rej.
CFT (a)	90	x3	99	x2
SVX+CFT	87	x5	99	x8

rate decreases from 117 to 16 Hz, i.e. a reduction by a factor 7. The number of selected $b \to J/\psi$ events is equal to 152 instead of 205, corresponding to a relative efficiency of 75%.

In summary, requiring STT tracks with a large impact parameter significance or asking for a good E_T/p_T matching lead to a significant background rate reduction for the DIELEC trigger. These two methods could serve different purposes, the first method being adequate to obtain a calibration sample and the second to select events suitable for physics analysis.

6 Update of Some Physics Studies

We have tried to reevaluate the feasibility of some B Physics studies in view of the trigger efficiency we can expect in Run II.

The B_s mixing studies [10] indicate that one needs to select B_s decay modes into all charged particles in the final state to achieve the proper time resolution necessary to measure the mixing parameter x_s in the $x_s > 15$ range. The most suitable decay modes for this decay are $B_s^\circ \to D_s^- + 3\pi^\pm$ $(\pi^\pm)$ followed by the D_s decay into $K^+K^-\pi^-$. The combined branching ratio for this mode is 3.8×10^{-4}.

The required number of detected events to make a 5σ measurement is $25/(\mathcal{D}^2 \times d_{time}^2)$, where $\mathcal{D}$ represents the total dilution factor excluding the effective dilution factor d_{time} due to time resolution. The expected $\mathcal{D}$ is 0.4, whereas the expected d_{time} decreases from 0.69 at $x_s = 10$ to 0.27 at $x_s = 20$. Therefore, we need to collect approximatively 600 and 2500 fully reconstructed B_s decays to measure x_s up to 15 and 20, respectively.

Our investigations indicate that with the XM2 trigger combined with the STT requirement (at least one track with $\mid S_B \mid > 2.5$) we expect to collect 25K such events in 2 fb^{-1} of data. The reconstruction efficiency is expected to be worse than 10% (12% of the B_s decay product have all final state particles with $p_T > 0.5$ GeV/c and $\mid \eta \mid < 1.5$). Therefore, the maximum number of reconstructed events will be 2500, at the border line for the $x_s = 20$ measurement. An efficient single muon trigger is our only chance for the B_s mixing measurement in the large x_s range.

The feasibility of studying the time integrated CP asymmetry with the DØ detector in Run II was addressed by Maciel and Lima in [2]. They used the MCfast Monte Carlo and estimated the number of expected fully reconstructed $B_d^\circ \to K_s + J/\psi$ events to 10K. This estimate is consistent with the Run 1 CDF experience of 2 reconstructed events per pb^{-1} of data. The expected number of events should allow to determine the $\sin 2\beta$ parameter with a precision of 0.12-0.15.

We have used our $K_s + J/\psi$ sample to confirm their findings. One event in this sample corresponds to a cross section of 1 pb $\times 8\,10^{-3}$, where the second factor represents the branching ratio for $b \to J/\psi\, K_s^0$, $K_s^0 \to \pi^+\pi^-$ relative to $b \to J/\psi\, X$. With the XM2 trigger we predict $2200 \times 2000 \times 8\,10^{-3} = 35$K triggered events. This number multiplied by the expected 30% K_s^0 reconstruction efficiency leads to 10K fully reconstructed events. Again, we have to stress that this could be an optimistic estimate and we can not afford to reduce our trigger efficiency.

7 Conclusions

We have presented a study of the signal efficiency and the background rate for single muon and dimuon triggers using various $b\bar{b}$ samples. Given the L1 and L2 bandwith limitations, the XM2 single muon trigger and the (XM1,XM2) dimuon trigger would give acceptable background rates together with the largest possible signal efficiency.

We have then investigated the benefits that would result from the use of a Silicon Track Trigger at L2. Despite the low multiplicity of charged particles in $b\bar{b}$ events, this device would allow to reduce the XM2 background rate by a factor 10 while preserving 70% of the reconstructable $Q\bar{Q}$ events. This result is marginally affected when a 30 μm smearing of the primary vertex position is taken into account. For the dimuon triggers, it would permit a reduction to 2 GeV/c of the p_T threshold on both muons, enriching the sample of signal events by 75% ($B_d^\circ \to K_s + J/\psi$) to 95% ($B_s^\circ \to D_s^- + \mu^+ + \nu_\mu$) compared to the (CM1,CM2) trigger and keeping the background rate as low as 10 Hz. If the XM2 background rate reveals to be acceptable, the trigger combination XM2.OR.[(CT1,CT1)+STT] allows a 33% increase of the trigger efficiency for $B_d^\circ \to K_s + J/\psi$ and $B_s^\circ \to D_s^- + \mu^+ + \nu_\mu$ events with respect to XM2 alone. This efficiency gain is accompanied by a moderate 16% increase of the background rate. The best compromise between background rate and efficiency is probably obtained with the combination [XM2.OR.(CT1,CT1)] +STT(2.5), which provides a 25.2% efficiency for $K_s + J/\psi$ events and leads to a background rate of 19.6 Hz, representing 2% of the L2 bandwith.

The STT would also be very useful to control the rate of a low threshold dielectron trigger, allowing the collection of low p_T $J/\psi \to ee$ events for calibration and physics analysis purposes.

Reevaluating the feasibility of some B Physics studies in Run II, we have shown that an efficient single muon trigger with $p_T \geq 4$ GeV/c is our only chance to search for B_s mixing up to $x_s = 20$ and to determine $\sin 2\beta$ with a competitive precision.

In summary, for all trigger configurations considered in this analysis, a Silicon Track Trigger would represent a powerful tool to reduce the background rates. From the physics analysis point of view, it would be more effective than a simple blind prescaling.

References

[1] For a review see, for instance, A.J. Buras and R. Fleischer, hep-ph/9704376.

[2] *A Study of CP Violation in the $B_d^\circ \rightarrow K_s + J/\psi$ Channel with the DØ Detector in Run II.*
G. Lima and A. Maciel, DØ note 3228 (March 1997).

[3] *The CDF and DØ B Physics Upgrades.*
A. Maciel, FERMILAB–Conf/97–214–E (1997).

[4] *A Vertex Trigger for Run II.*
F. Borcherding *et al.*, DØ note 2984 (June 1996).

[5] M. Mangano, P. Nason and G. Ridolfi, Nucl. Phys. **B373**, 295 (1992).

[6] K. Johns, private communication.

[7] *Benefits of a Silicon Vertex Trigger for $t\bar{t}$ Events.*
F. Stichelbaut, DØ note 3312 (September 1997).

[8] A. Zieminski, Proceedings of the XXXIst Rencontres de Moriond, March 1996, p.241.

[9] F. Abe *et al.*, CDF Collaboration, Phys. Rev. Lett., **79**, 572 and 578 (1997).

[10] D. Ritchie, J. Skarha and A. Zieminski, Proceedings of Snowmass 1993, p.357.

Appendix A: Trigger Definition

The definition of the various triggers used in this analysis is the following:

- **MUMAX1**
  - L1: at least 1 XL μ with $p_T^\mu \geq 7$ GeV/c
  - L2: at least 1 CFT track with $p_T \geq 6$ GeV/c
- **MUMAX2**
  - L1: at least 1 XT μ with $p_T^\mu \geq 7$ GeV/c
  - L2: at least 1 CFT track with $p_T \geq 6$ GeV/c
- **DIMU1**
  - L1: at least 2 XL μ's with $p_T^\mu \geq (2,4)$ GeV/c
  - L2: at least 2 CFT tracks with $p_T \geq 4$ GeV/c
- **DIMU2**
  - L1: at least 2 XT μ's with $p_T^\mu \geq (2,4)$ GeV/c
  - L2: at least 2 CFT tracks with $p_T \geq 4$ GeV/c
- **MUJET**
  - L1: at least 1 XL μ with $p_T^\mu \geq 1.5$ GeV/c and 2 jets with $E_T > 5$ GeV
  - L2: at least 1 XL μ with $p_T^\mu \geq 7$ GeV/c, 1 jet with $E_T > 20$ GeV and 1 jet with $E_T > 10$ GeV
- **DIMUJ**
  - L1: at least 2 XL μ's with $p_T^\mu \geq 2$ GeV/c and 1 jet with $E_T > 5$ GeV
  - L2: at least 1 jet with $E_T > 10$ GeV
- **DIELEC**
  - L1: at least 2 EM towers with $E_T > 2.5$ GeV
  - L2: at least 2 EM clusters with $E_T > 3$ GeV

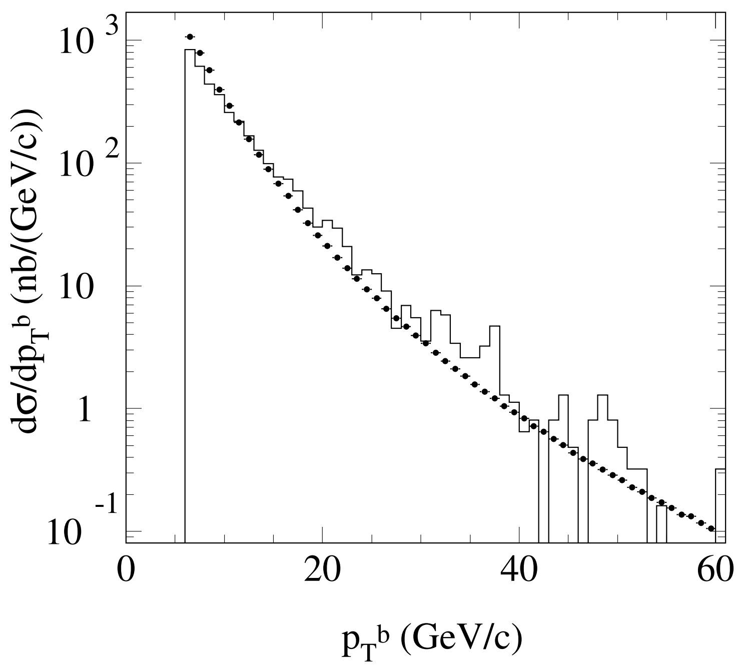

Figure 1: Comparison of the p_T^b spectrum predicted by ISAJET (open histogram) and MNR (closed points) for $|\ y^b\ | < 1$. The ISAJET spectrum is normalised to the MNR prediction for the integrated cross section when $p_T^b > 6$ GeV/c.

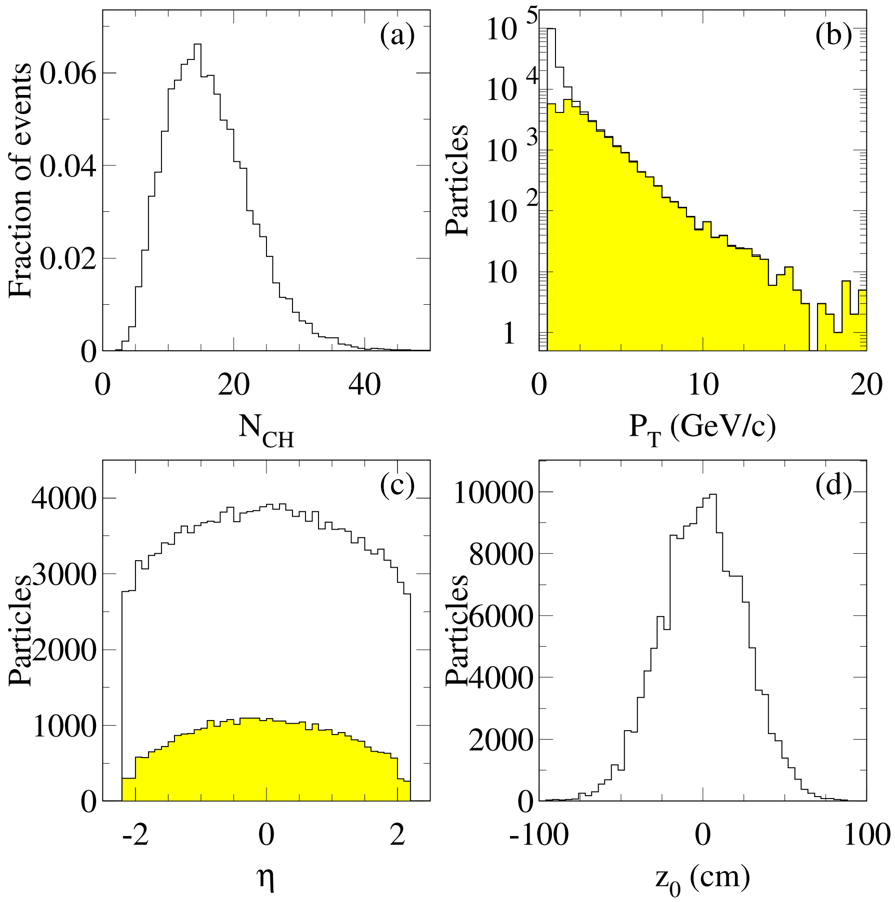

Figure 2: Some properties of $B_d^\circ \to K_s + J/\psi$ events: (a) Multiplicity of charged particles with $p_T > 0.5$ GeV/c and $\mid \eta \mid \leq 2.2$; (b) p_T spectrum for all charged particles (open histogram) and those coming from the decay of B mesons (shaded histogram); (c) η distribution for all charged particles (open histogram) and particles produced in B meson decays (shaded histogram); (d) distribution of the z coordinate of the point of origin of all charged particles (primary or secondary vertex).

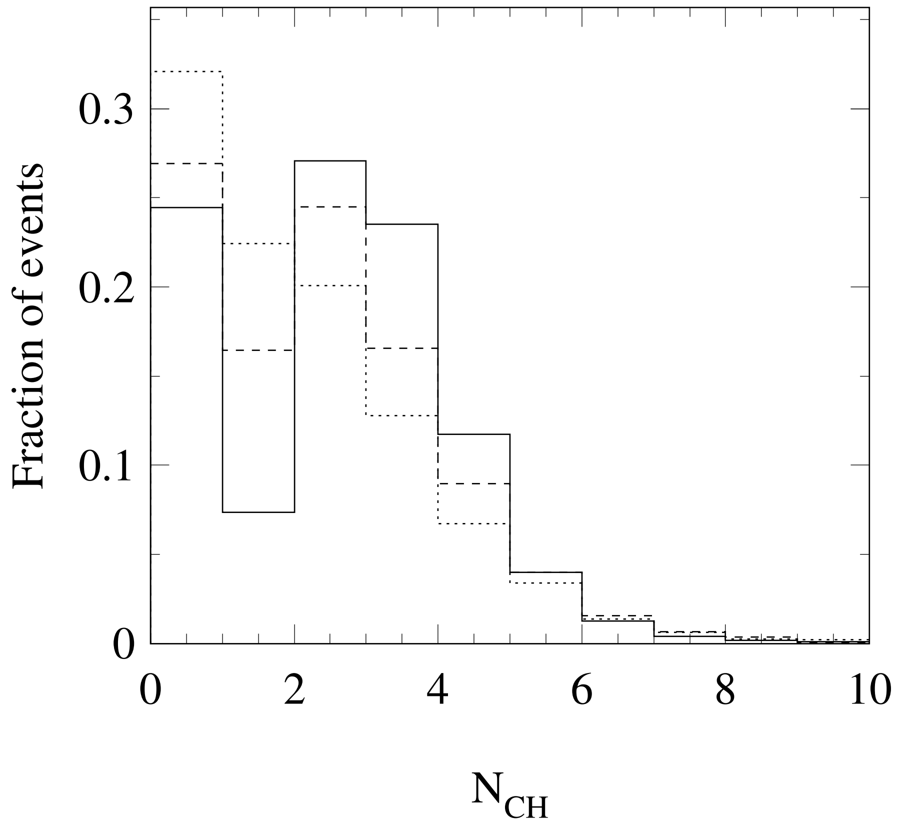

Figure 3: Multiplicity of charged particles with $p_T > 1.5$ GeV/c, $\mid \eta \mid \leq 1.6$ and $\mid z_0 \mid \leq 30$ cm. The open histogram corresponds to the $B^\circ_d \rightarrow K_s + J/\psi$ events, the dashed histogram to the $B^\circ_s \rightarrow D^-_s + \mu^+ + \nu_\mu$ events and the dotted histogram to the $B^\circ_s \rightarrow D^-_s + 3\pi^\pm$ events.

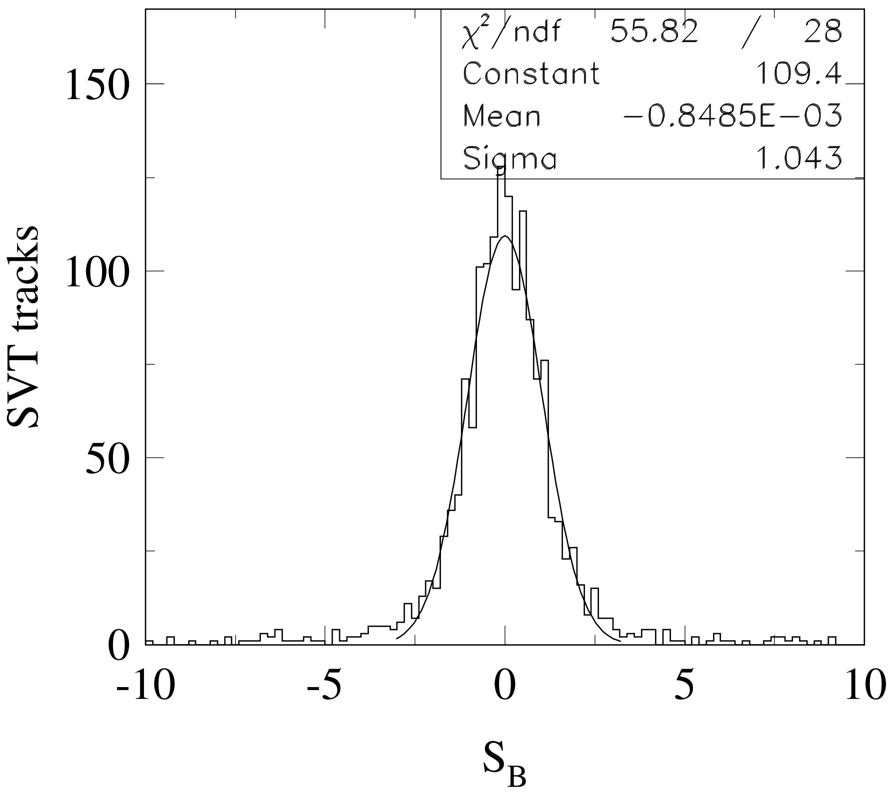

Figure 4: Impact parameter significance distribution for STT tracks coming from the primary vertex after quality cuts.

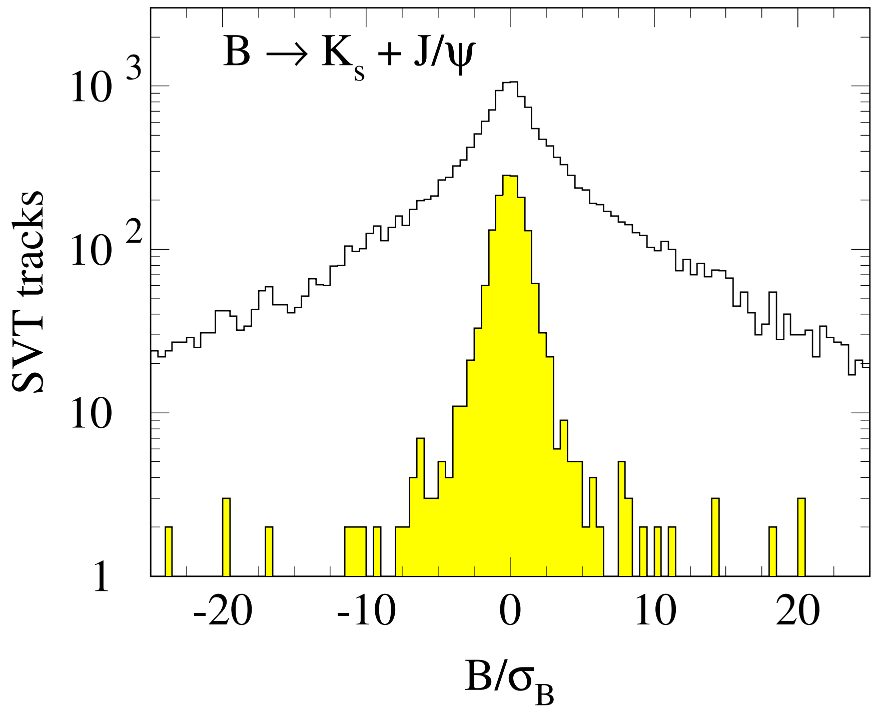

Figure 5: Significance distribution for STT tracks reconstructed in $B_d^\circ \rightarrow K_s + J/\psi$ events. The open histogram corresponds to all the matched tracks while the shaded histogram only contains the matched tracks coming from the primary vertex.

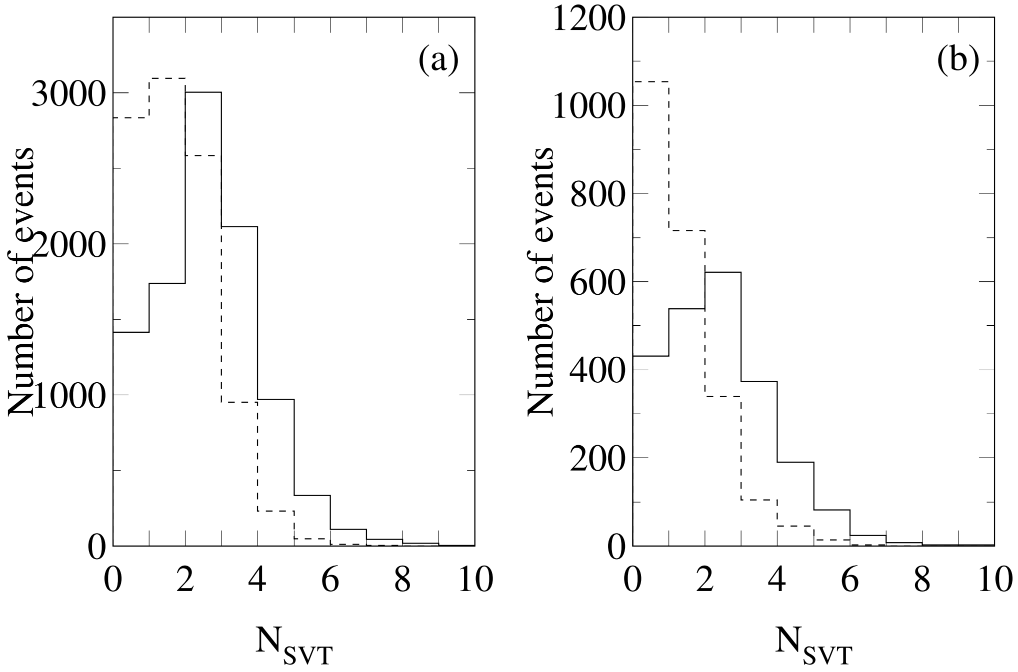

Figure 6: Multiplicity of STT tracks after the track quality cuts (open histogram) and after requiring an absolute significance greater than 2 (dashed histogram): (a) $B_d^{\circ} \rightarrow K_s + J/\psi$ events; (b) $B_s^{\circ} \rightarrow D_s^- + \mu^+ + \nu_\mu$ events.

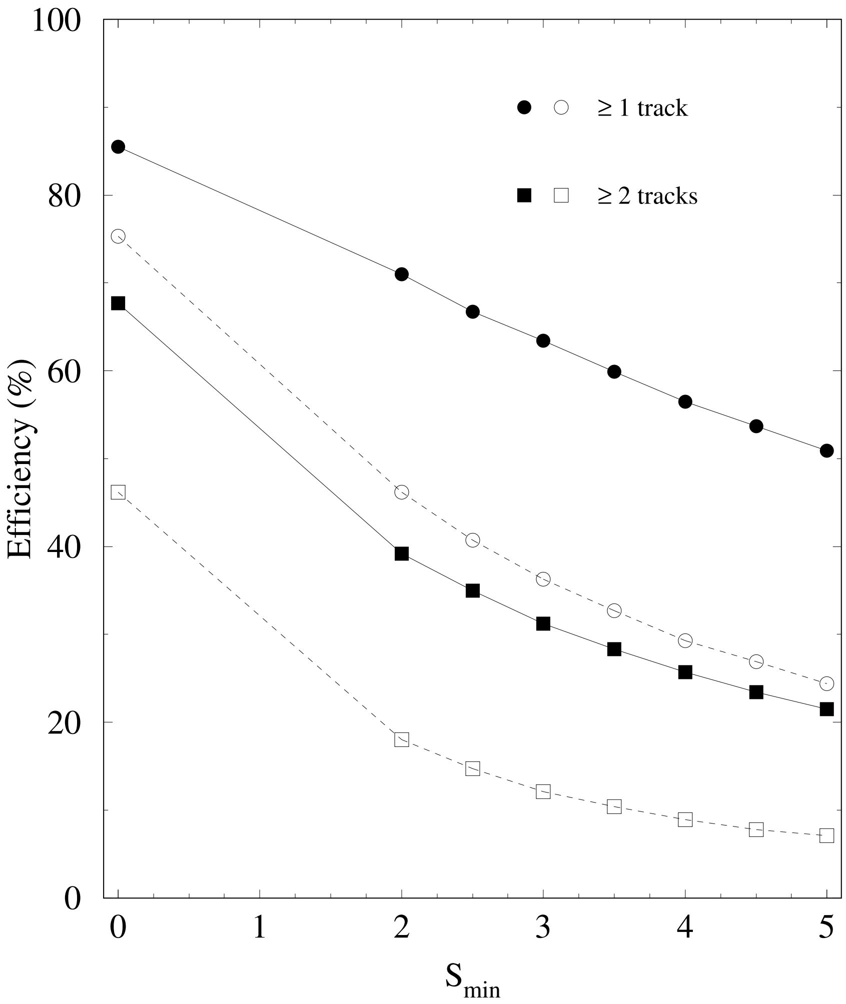

Figure 7: STT efficiency for $B_d^\circ \to K_s + J/\psi$ (closed symbols) and $B_s^\circ \to D_s^- + 3\pi^\pm$ events (open symbols).

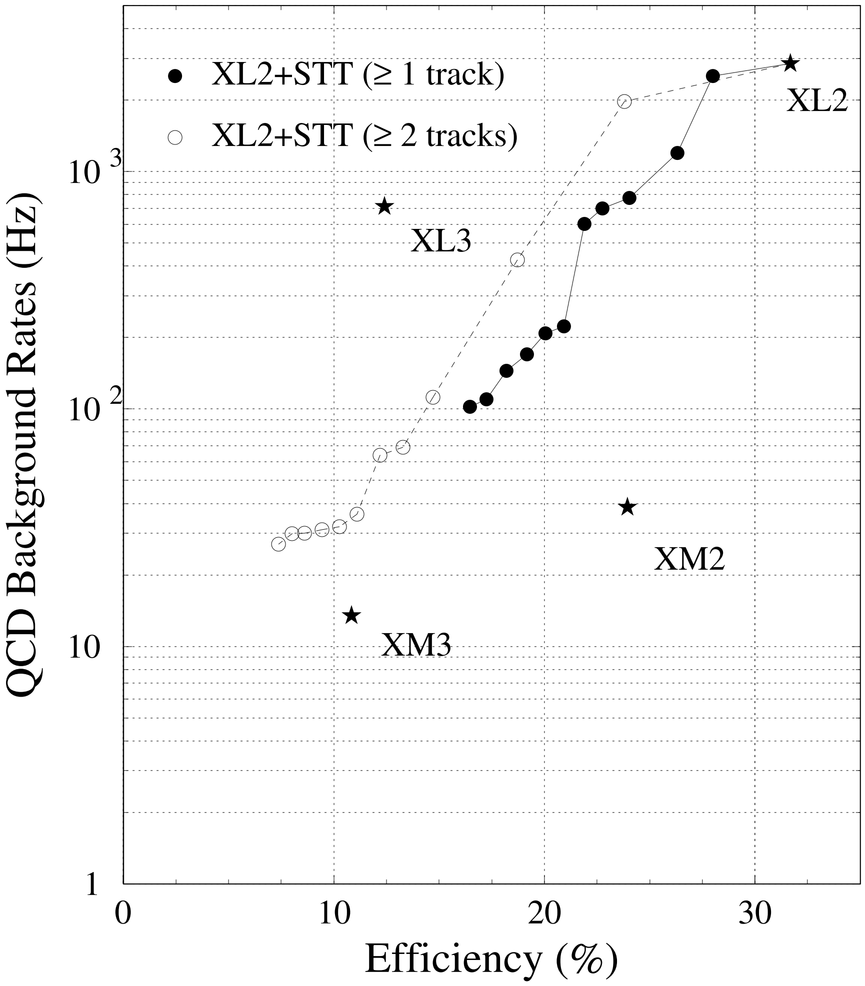

Figure 8: Efficiency for $B_d^\circ \rightarrow K_s + J/\psi$ events versus background rate for various single muon triggers.

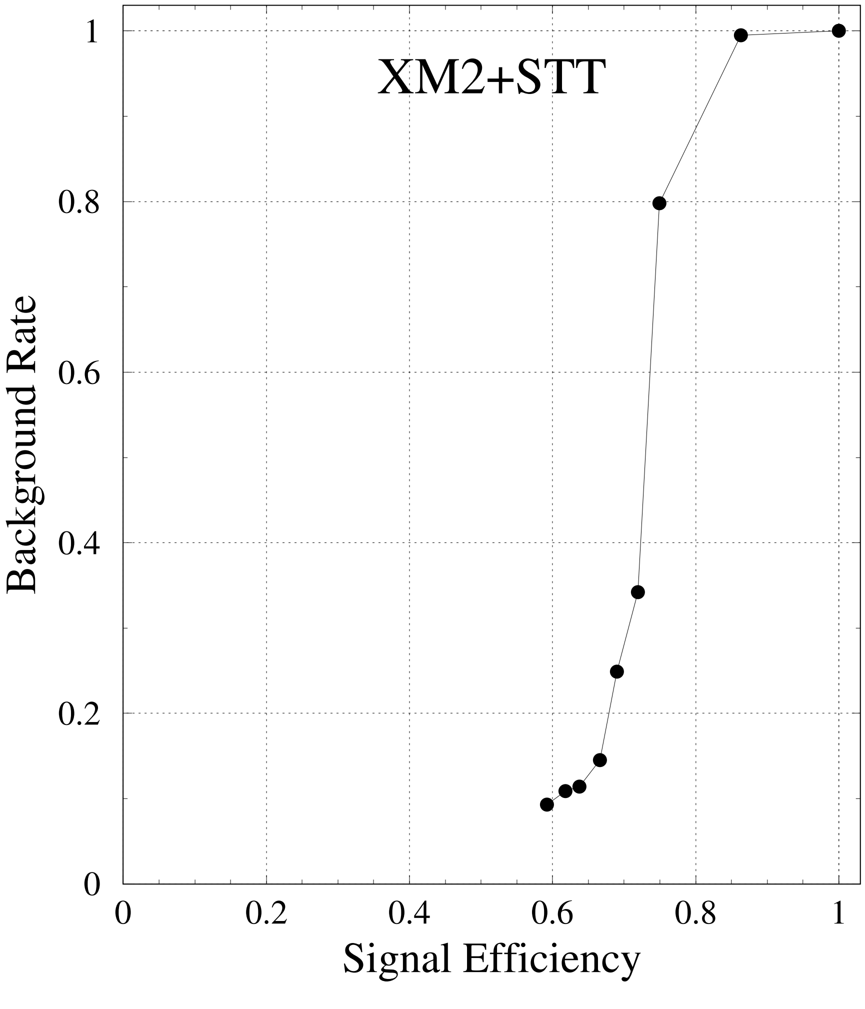

Figure 9: Efficiency for $Q\bar{Q}$ events versus background rate for XM2+STT trigger.

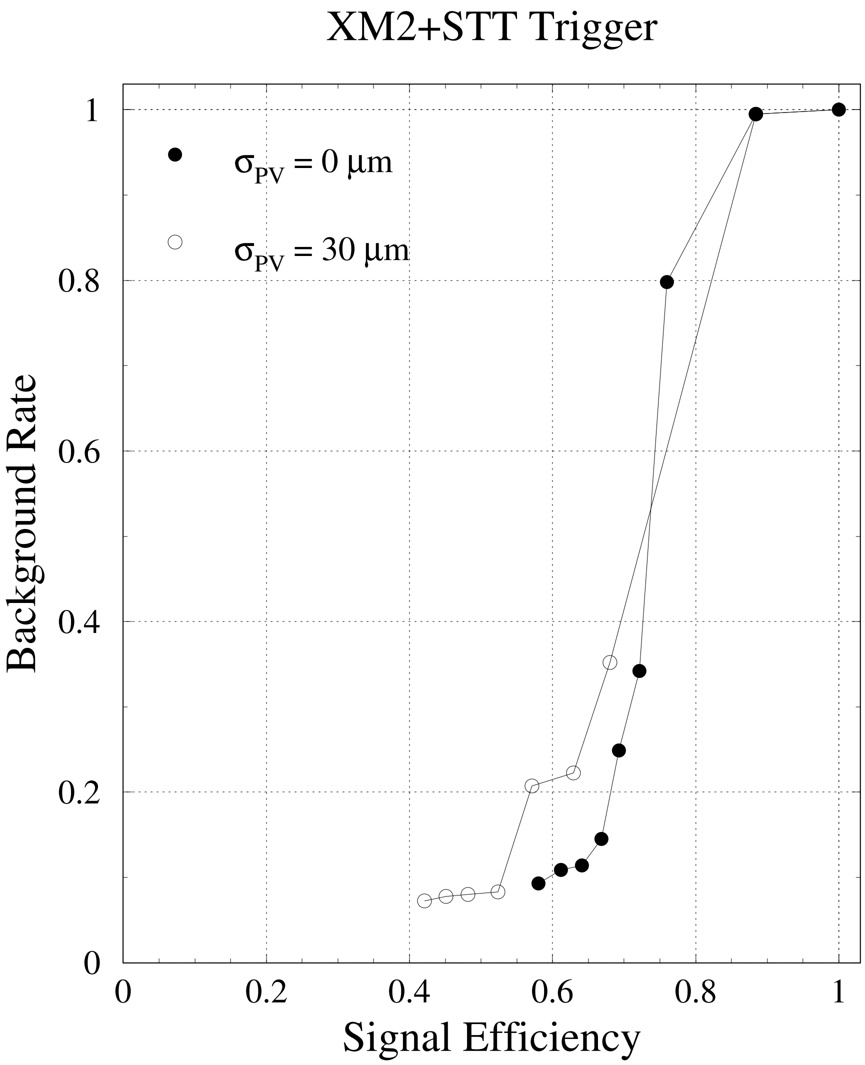

Figure 10: Efficiency for $B_d^\circ \rightarrow K_s + J/\psi$ events versus background rate for the XM2+STT trigger, without smearing of the primary vertex position (closed circles) and with a smearing of 30 μm (open circles).

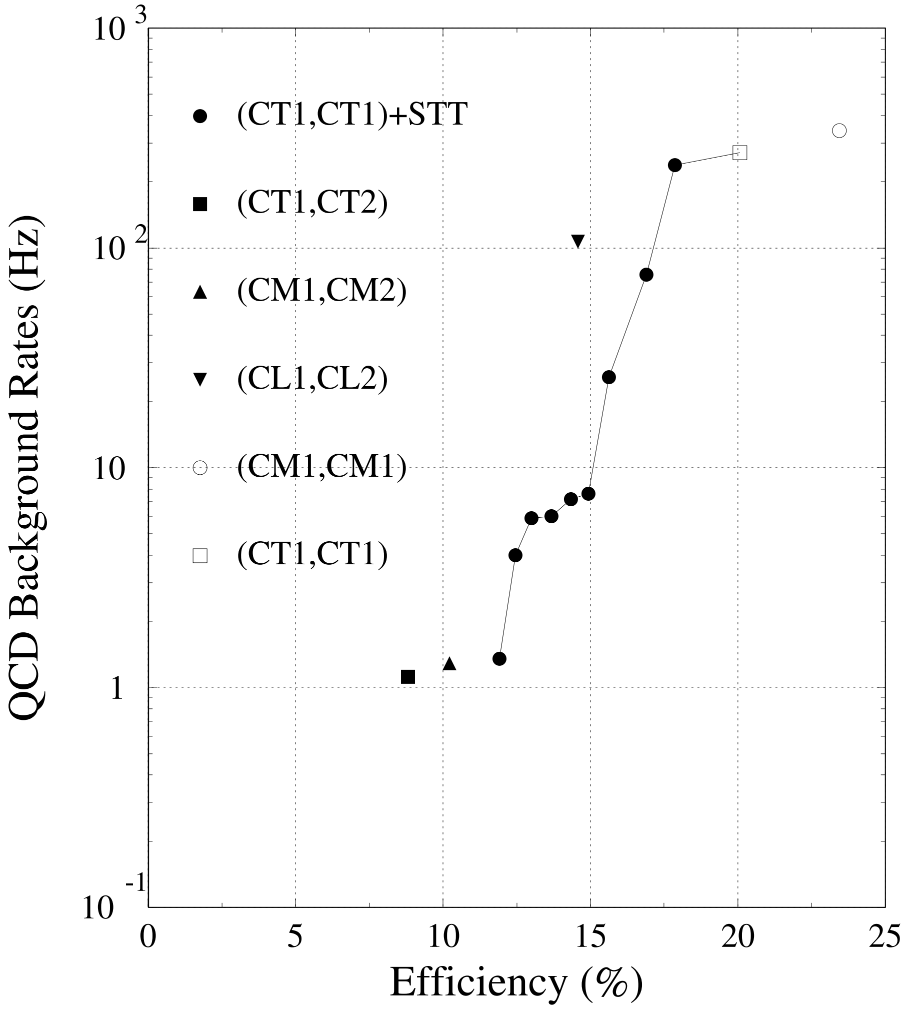

Figure 11: Efficiency for $B_d^\circ \rightarrow K_s + J/\psi$ events versus background rate for various dimuon triggers.

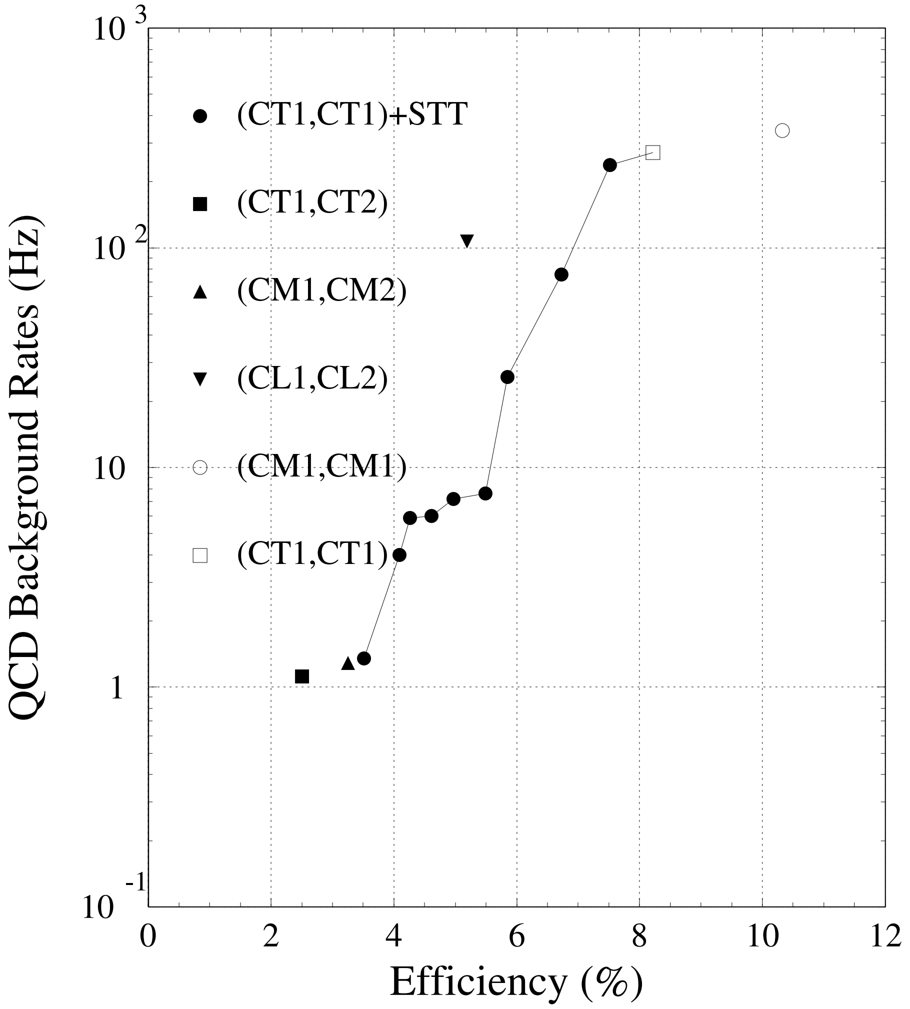

Figure 12: Efficiency for $B_s^\circ \rightarrow D_s^- + \mu^+ + \nu_\mu$ events versus background rate for various dimuon triggers.

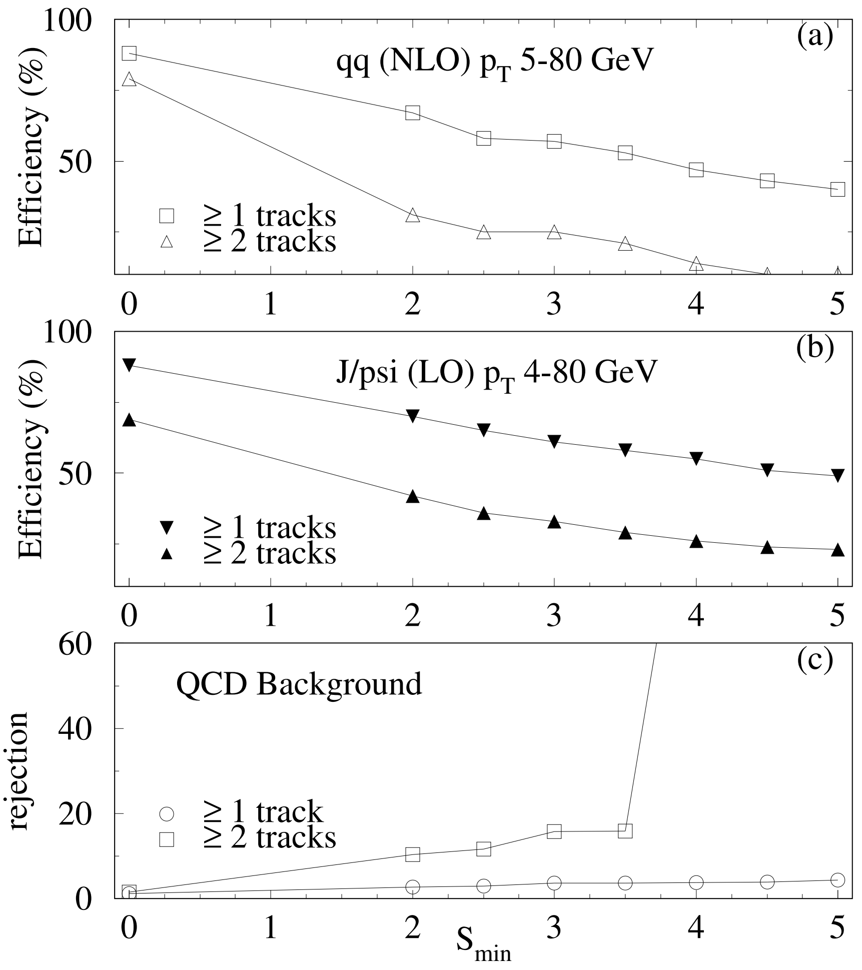

Figure 13: Efficiency of the DIELEC+STT trigger for (a) $Q\bar{Q} \rightarrow ee$ and (b) $J/\psi \rightarrow ee$ events. The background rejection factors for this trigger are shown in (c).

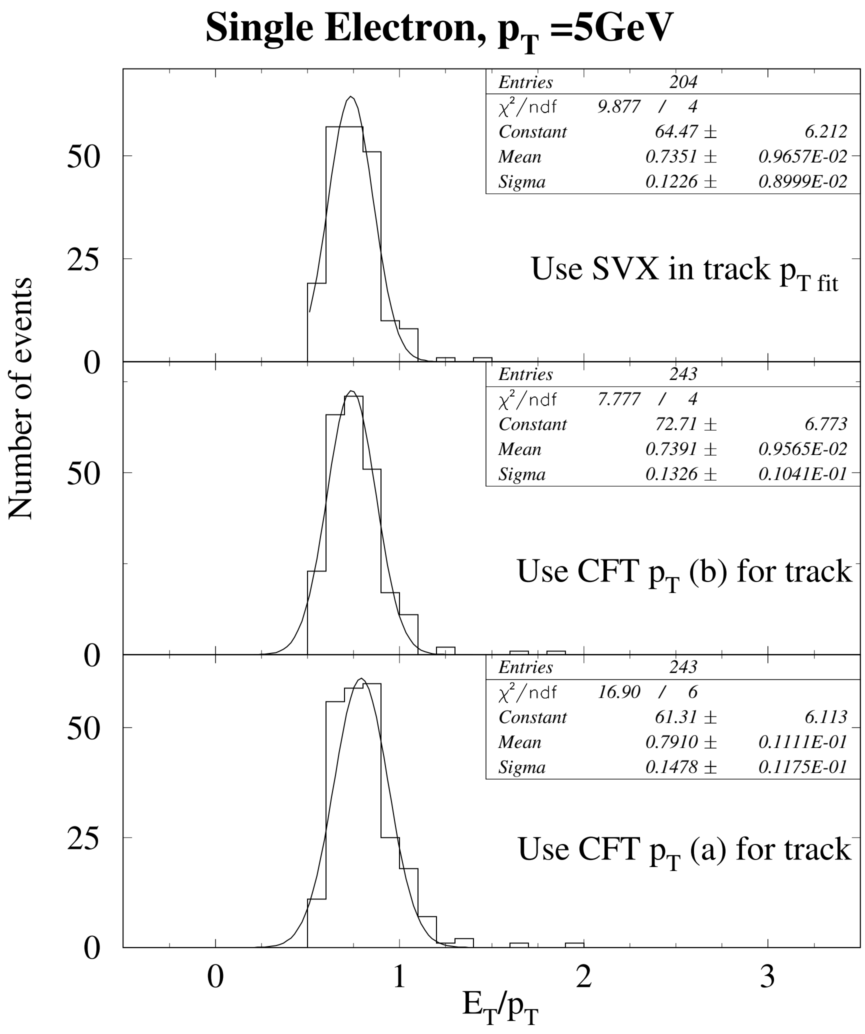

Figure 14: E_T/p_T distributions obtained from 5 GeV single electron events: (a) using the SVX information; (b) using definition (b) for CFT-p_T; (c) using definition (a) for CFT-p_T.

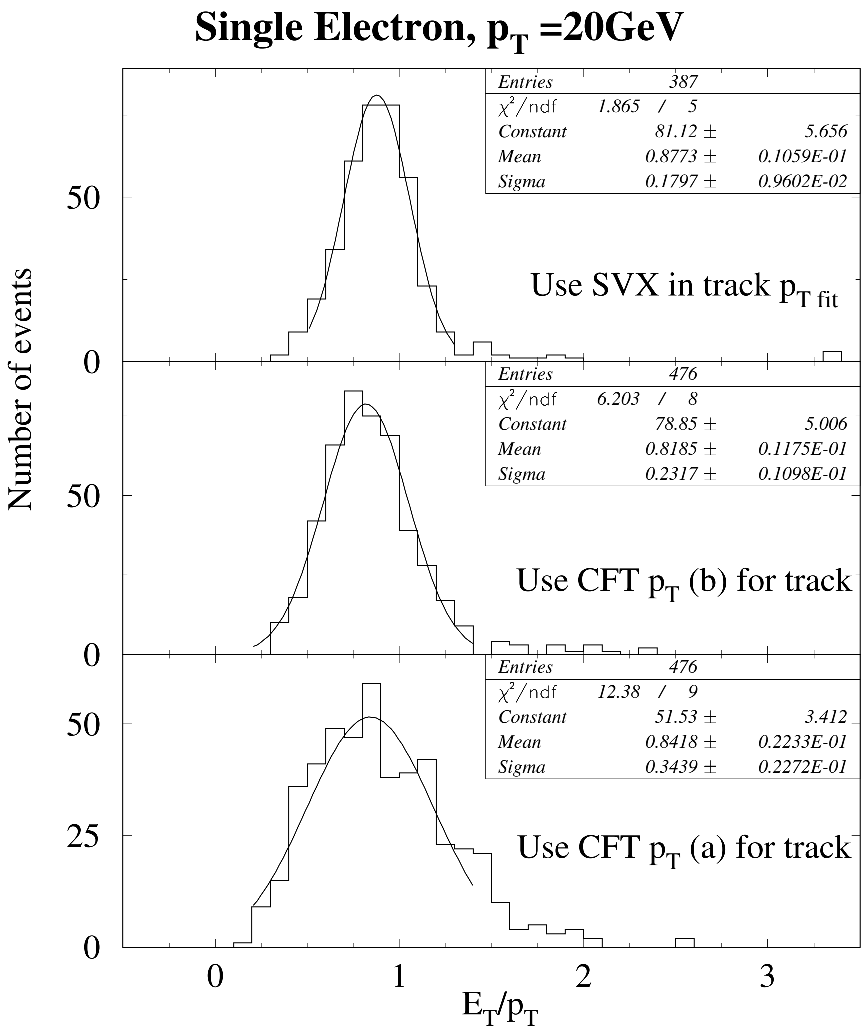

Figure 15: E_T/p_T distributions obtained from 20 GeV single electron events: (a) using the SVX information; (b) using definition (b) for CFT-p_T; (c) using definition (a) for CFT-p_T.